Performance measurement of a PET insert using strip-line readout and waveform sampling data acquisition for simultaneous PET/MRI

Heejong Kim, Yuexuan Hua, Daoming Xi, Qingguo Xie, Hsiu-Ming Tsai
Hsing-Tsuen Chen, Xiaobing Fan, Gregory Karczmar, Chin-Tu Chen, Cheng-Ying Chou, Chien-Min Kao

***Abstract*—Previously we reported the development of a PET insert for PET/MRI using strip-line signal readout and waveform sampling data acquisition for small animal imaging. Based on encouraging results obtained from the previous prototype, we have made several major upgrades for improvement. Firstly, the number of detector modules were increased from 8 to 14 to increase sensitivity and eliminate image artifacts. Each detector module consists of 8x4 LYSO arrays (3x3x10 mm^3 each) and two Hamamatsu S13361-3050NE-04 MPPC arrays (4x4, 3.2 mm pitch). The detector modules are installed within a 3d-printed plastic supporting structure with 60 mm inner diameter and 115 mm outer diameter to fit inside 9.4 Tesla Bruker BioSpec 94/30 USR MR scanner. The axial field of view of the PET insert is 25.6 mm. Secondly, the SiPM signal readout multiplexing ratio is increased double in the detector module by redesigning the strip-line board;32 SiPM signals from MPPC arrays are routed to 2 strip-lines so that 16 LYSO/SiPMs send outputs to a common strip-line for readout. Experiments using the PET insert have been conducted inside and outside an MR scanner for performance evaluation. The mutual interferences of the integrated system are assessed by comparing PET and MR images of a custom-made resolution phantom. Preliminary test results are very promising and demonstrate that detector design based on strip-line signal readout is suitable for PET/MR system. We present the development of the PET insert and the preliminary experimental results.**

I. Introduction

Previously we reported the development of a PET insert for PET/MRI [1] using strip-line readout and waveform sampling data acquisition (DAQ) for small animal imaging. In strip-line readout [2] [3], multiple SiPMs send outputs to a common strip-line, and position information of a hit SiPM is encoded in the signal propagation time difference along the strip-line. With this readout it is possible to position the DAQ remotely; therefore, the detection module within MR can be kept minimal and compact while also greatly mitigate the concerns for generation of RF signals and heat. These features are advantageous in developing PET/MR integrated system. Based on encouraging results obtained from the previous prototype, we have made several major upgrades for improvement. The strip-line readout board, which is a key component of detector module, has been redesigned to increase the SiPM signal multiplexing ratio two times. To increase sensitivity and eliminate image artifacts (or the need for rotation), the number of detection modules were increased from 8 to 14, and the gaps between detector modules are now significantly reduced. Experiments using the insert have been conducted inside and outside a 9.4T small-animal MR scanner to measure performance.

Heejong Kim, Hsiu-Ming Tsai, Hsing-Tsuen Chen, Xiaobing Fan, Gregory Karzmar, Chien-Min Kao, and Chin-Tu Chen are with the Department of Radiology, University of Chicago, IL, US

Yuexuan Hua, Daoming Xi and Qingguo Xie are with Biomedical Engineering Department, Huazhong University of Science and Technology, Wuhan, China

Cheng-Ying Chou is with Department of Bio-Industrial Mechatronics Engineering, National Taiwan University, Taipei, Taiwan

II. Material and Methods

A detector module consists of a strip-line board (SLB) and 8x4 LYSO scintillator array (each LYSO 3x3x10mm^3). Two units of Hamamatsu S13361-3050NE-04 MPPC array (4x4, 3.2 mm pitch) are used in each detector module, and 32 SiPMs output signals are routed to 2 strip-lines (SL). SiPM and LYSO in arrays is coupled one to one (1:1). Fig. 1(1) shows a strip-line board and a detector module with the LYSO array installed. The insert, shown in Fig. 1(2, 3), contains 14 detector modules; the detector modules are installed inside a 3d-printed plastic supporting structure having 60 mm inner diameter and 115 mm outer diameter. The axial field-of-view of the detector is $\sim$25.6 mm. The output signals (total 56) of 14 detector modules are fed to a multi-threshold voltage (MVT) digitizer board [4] (Raycan Technology, China) through 5 m long coaxial cables with MMCX connector. The MVT board, shown in Fig. 1(4), samples an input signal at 4 user defined voltages, obtaining time values of the samples using time-to-digital converters (TDC). This sampling method is implemented using Altera EP4C115F29C7 FPGAs, and the digitized samples are sent through a gigabit Ethernet and stored for off-line analysis. The TDC bin resolution is $\sim$100 ps. The dimension of the insert is constrained by the 9.4 Tesla small animal MR scanner (Bruker BioSpec 94/30 USR) [5]. Currently, four voltage thresholds are set to 50, 150, 300, and 600mV. For performance evaluation, a 19 cm long ^{68}Ge rod source (ID=3mm, $\sim$100μCi activity) was placed at the trans-axial center of the insert. The data were also collected at several off-center positions (5, 10, 15, 20, and 25 mm) for the rod source. A custom-made resolution phantom with hole diameters ranging from 1.0 mm to 3.0 mm was filled with liquid ^{18}F, and data were acquired for assessing image

978-1-5386-8494-8/18/$31.00 ©2018 IEEE

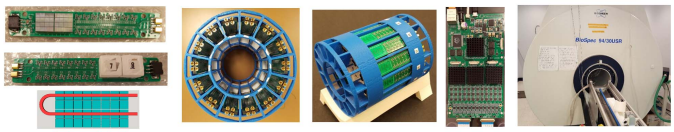

Figure 1: (1) Detector module consisting of strip-line board and LYSO arrays. (2, 3) A PET insert assembled with 14 detector modules. (4) 72 input channel MVT digitizer board. (5) A Bruker BioSpec 94/30 USR MR scanner for the insert.

resolution. MR images were acquired before and after placing the insert inside the MR scanner to investigate the effects of PET to MRI.

III. Preliminary Results

Fig. 2(1) shows the recovery of the signal pulse, demonstrating a good fitting result using an bi-exponential function [4]. The histogram of arrival time difference on a strip-line is shown in Fig. 2(2). The four time-stamps on the rising part of signal pulse are averaged for calculating time difference. The interaction position on strip-line is determined based on the time difference histogram; the 16 peaks in the histogram represents represent the positions of the 16 SiPMs on a strip line. The average peak/valley ratio in this histogram is measured to ∼15 for the entire insert. The energy of the event

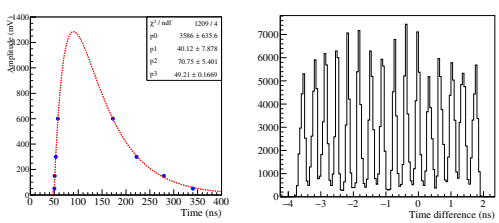

Figure 2: (1) Pulse shape reconstruction by exponential fitting (red curve) to the MVT samples (blue solid circles) (2) The differential time histogram on a strip-line. Each peak of the histogram corresponds to one SiPM.

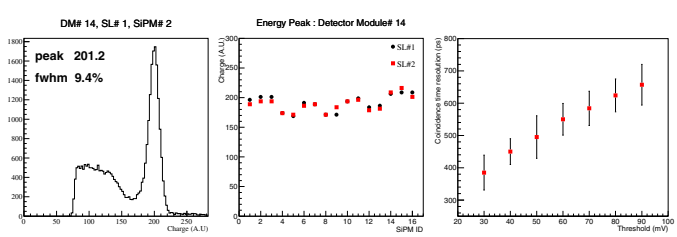

Figure 3: (1) Pulse height spectrum of a LYSO/SiPM based on the area of the fitted curve. (2) Pulse height corresponding to 511 keV for each LYSO/SiPM in two strip-lines in a detector module. (3) Coincidence time resolution for two selected detector modules, as a function of the threshold used for event time determination (the lowest of the MVT thresholds).

is estimated by integrating the area under the fit function, and Fig. 3(1) shows an example energy spectrum obtained for a LYSO/SiPM. The overall gain of detector module is found to be rather uniform as illustrated by Fig. 3(2). The average energy resolution of a detector module at 511 keV is measured to be ∼10%. For measuring event time, the time-stamp of the lowest threshold is used; the best coincidence time resolution is obtained with the lowest threshold time-stamp. The averaged coincidence time resolution (CTR) of two selected detector modules as a function of the lowest threshold is shown in Fig. 3(3). For the entire insert, the CTR is measured to be ∼500 ps FWHM. It is important to note that when using DRS4 waveform sampler [6] to acquire the signal at 2.5 GS/s sampling rate, the CTR has been measured to be ∼265 ps. Therefore, the inferior ∼500 ps CTR is limited by the intrinsic timing resolution of the MVT board. Image reconstruction uses a maximum-likelihood

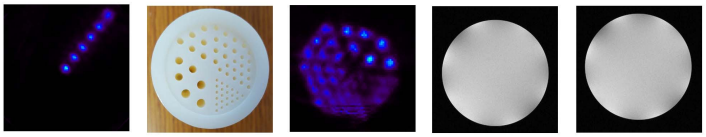

Figure 4: (1) ^{68}Ge line source images at different locations (5, 10, 15, 20, and 25 mm from the center). (2) A custom-made resolution phantom (Hole diameters are 1.0, 1.4, 1.8, 2.2, 2.6, and 3.0 mm, respectively). (3) PET image of the resolution phantom, filled with ^{18}F solution. (4) MR image acquired before introducing the insert inside the MR scanner. (5) MR image acquired after inserting PET.

expectation maximization (MLEM) algorithm, and corrections for detection efficiency and attenuation are not included yet. The reconstructed images (144x144x52, 0.5 mm pixels) of the ^{68}Ge rod source is shown in Fig. 4(1). The system response matrix for image reconstruction is calculated by using Siddon's ray tracing and is calibrated by the ^{68}Ge line source images. The custom-made resolution phantom and image using ^{18}F are shown in Fig. 4(2, 3). The holes with diameter 1.8 mm is well resolved in the image. The effects on MR due to PET were tested by acquiring MR image of an uniform phantom filled with water before and after placing the insert into the MR scanner. The T1 weighted gradient echo images of a water phantom (diameter 25.6 mm) are shown in Fig. 4(4, 5). No image artifacts are observed after the insert is introduced.

Acknowledgment

This work was supported in part by the University of Chicago Medicine Comprehensive Cancer Center pilot award, Ministry of Science and Technology #MOST 106-2221-E-002-080, the National Natural Science Foundation of China (NSFC) Grant #61425001, #61671215, #61604059, the National Key Scientific Instrument and Equipment Development Project of China #2013YQ030923, and the National Key Research and Development Program #2016YFF0101501. The authors thank the Hamamatsu Corporation for providing the S13361-3050NE-04 MPPC arrays used in this study.

References

[1] H. Kim et. al, IEEE NSS/MIC conference (2017) M-07-3.

[2] H. Kim et. al, Nucl. Instr. and Meth. **830** (2016) 119.
[3] H. Kim et. al, Nucl. Instr. and Meth. **784** (2015) 557.
[4] X. Mei et al., IEEE NSS/MIC Conference Record (2014) DOI:10.1109/NSSMIC.2014.7431224
[5] http://www.bruker.com/products/mr/preclinical-mri/biospec/technical-details.html
[6] S. Ritt, R. Dinapoli, U. Hartmann, NC. Instr. and Meth. **623** (2010) 486.